EUROPEAN ORGANIZATION FOR NUCLEAR RESEARCH

CERN-EP/83-83
21 June 1983

OBSERVATION OF $D^{*\pm}$ AND $(\bar{D})^0/D^{\pm}$ PRODUCTION IN HIGH-ENERGY π^-Be INTERACTIONS AT THE SPS

ACCMOR Collaboration

Amsterdam[1]-Bristol[2]-CERN[3]-Cracow[4]-Munich[5]-Rutherford[6] Collaboration

R. Bailey[6], D.G. Bardsley[2], H. Becker[5], G. Blanar[5], T. Böhringer[3], M. Bosman[3], M. Cerrada[3], V. Chabaud[3], C. Damerell[6], C. Daum[1], H. Dietl[5], H. Dijkstra[1], A. Dwurazny[4], W. Faissler[5*], M. Gettner[5*], D. Giddings[6], A. Gillman[6], R. Gilmore[2], L. Görlich[5**], Z. Hajduk[4], C. Hardwick[6], L.O. Hertzberger[1], W. Hoogland[1], B.D. Hyams[3], R. Jongerius[1], R. Klanner[5], E. Lorenz[5], G. Lütjens[5], G. Lutz[5], J. Malos[2], W. Männer[5], G. Polok[1**], M. Rozanska[4], K. Rybicki[4], T.W.L. Sanford[5], H.J. Seebrunner[5], P. Sharp[6], W. Spierenburg[1], U. Stierlin[5], R.J. Tapper[2], H.G. Tiecke[1], M. Turala[4], J.C. Vermeulen[3], G. Waltermann[5], P. Weilhammer[3], R.J. Whyley[2], F. Wickens[6], L.W. Wiggers[1], A. Wylie[3] and T. Zeludziewicz[5**]

ABSTRACT

An experiment has been performed to search for associated hadronic production of charmed mesons, using a large-aperture forward magnetic spectrometer set-up in a π^- beam at the CERN SPS. A prompt electron trigger was used to select events containing a pair of charmed particles. D mesons have been identified by reconstruction of hadronic decay modes such as $K\pi$, $K\pi\pi$. Data have been taken at 120, 175, and 200 GeV. The $D\bar{D}$ cross-section measured at 175/200 GeV is $\sigma(D\bar{D}) = (48 \pm 15)\mu b$ with a systematic uncertainty of ±50%. The energy dependence of the cross-section is measured to be $\sigma(D\bar{D})[120\ GeV]/\sigma(D\bar{D})[175/200\ GeV] = 0.62 \pm 0.34$.

(Submitted to Physics Letters)

---

1) NIKHEF-H, Amsterdam, The Netherlands.
2) University of Bristol, Bristol, UK.
3) CERN, Geneva, Switzerland.
4) Institute of Nuclear Physics, Cracow, Poland.
5) Max Planck Institut für Physik, Munich, Fed. Rep. Germany.
6) Rutherford Laboratory, Chilton, Didcot, UK.
*) Visitor from Northeastern University, Boston, Mass., USA.
**) Visitor from Institute of Nuclear Physics, Cracow, Poland.

1. INTRODUCTION

After the discovery of charmed particles in e^+e^- interactions at SPEAR [1], the study of hadroproduction of charm has been actively pursued in recent years at the CERN ISR and at the high-energy proton accelerators at FNAL and CERN. In hadroproduction the absolute charm production rate is high -- approximately 200 charm events per SPS burst in this experiment -- thus allowing, in principle, a detailed study of the production mechanism and decay properties of particles containing a charm quark. In practice, however, owing to the large ratio of inelastic cross-section to charm cross-section, and high multiplicities, resulting in large combinatorial background, no experiment so far has managed a high statistics study of charmed particles in hadronic interactions.

A number of results have been obtained up to now on D and Λ_c production. The following types of experiments can be distinguished: experiments indirectly measuring charm production by detecting prompt leptons assuming that these come from semileptonic charm decays [2]; experiments looking for secondary vertices due to charm decays, using the relatively long lifetimes of charmed particles ($\sim 10^{-13}$-10^{-12} s) [3,4]; experiments looking directly for charm signals in invariant mass spectra [5]. In this last type of experiment an improvement in signal-to-background ratio is achieved either by observing cascade decays [6] or by tagging on a prompt lepton from the semileptonic decay of one of a pair of charmed particles [7].

In this letter we report on results of the experiment NA11 in the H6 beam at the CERN SPS, in which we have investigated charm production in 120 to 200 GeV π^-Be interactions using a prompt electron trigger. We present results on the observation of $D^{*\pm}$, $D^{\pm}$, D^0, and $\bar{D}^0$ mesons in mass spectra and a determination of the cross-section. Properties of the production mechanism and of decays will be discussed in an accompanying letter [8].

2. THE EXPERIMENT

The experiment was designed to select inelastic π^-Be interactions where a pair of charmed particles ($D\bar{D}$, $D\bar{D}^*$, $D\bar{F}$, ...) is produced by tagging on the electron

coming from the semileptonic decay of one of the particles and measuring the hadronic decay modes of the other, e.g.

$$\pi^- Be \to D^0 \quad + \bar{D}^0 \quad + X \ .$$
$$\hookrightarrow K^-\pi^+ \qquad \hookrightarrow e^- K^0 \nu$$

The forward-going hadronic system is measured in a large-acceptance forward magnetic spectrometer [9] (fig. 1a). The main components of the spectrometer are two magnets M1 (0.9 T·m) and M2 (2.0 T·m), 48 planes of large drift chambers arranged in 4 packs (Arm 2 - Arm 3c), 3 multicellular Čerenkov counters (C1, C2, C3) for particle identification, and a photon calorimeter (γ-CAL).

The equipment used for triggering and off-line selection of single electrons is shown in fig. 1b. It consists of electromagnetic calorimeters, threshold Čerenkov counters, and multiwire proportional chambers (MWPCs). The two segmented Pb-scintillator calorimeters (E-CAL) are mounted above and below the aperture of magnet M2, covering from 50 to 150 mrad above and below the beam line. Matching the acceptance of the electron calorimeters, there are two segmented threshold Čerenkov counters (Q) with a pion threshold of 12 GeV, installed inside the gap of magnet M1. A system of MWPCs is mounted inside the gap of M1 (P1, P8, and P9) and between M1 and M2 (P2A, P2B). Four 8 mm long Be targets with a height of 2 mm and a width of 20 mm are used. The targets are segmented and small in height in order to minimize photon conversion within the solid angle of the electron trigger equipment.

The fast trigger demands an interaction in one of the targets, a signal in the Čerenkov counter Q, together with a geometrically correlated shower in the calorimeter, and the absence of a coplanar electron from photon conversion in the calorimeter or in a set of Pb-scintillator veto counters H.

In a second stage trigger two ESOP microprocessors [10] are used to reject further background. The momentum p_e and energy E_e of the trigger particle are determined respectively from the corresponding hits in the MWPCs P2A and P2B and the pulse-height information from the calorimeter. The following cuts are applied: $3\ \text{GeV} < p_e < 12\ \text{GeV}$, $0.7 < E_e/p_e < 1.3$, and $p_{Te} > 0.3\ \text{GeV}$, where p_{Te} is the transverse momentum of the electron. Furthermore, electron pairs from

conversions in which the pair electron reaches the P2B chamber are rejected by the microprocessors. The average processing time per event sent to the microprocessors is 500 μs. Two NORD 10 on-line computers are used to monitor the experiment and write the data to tape. The data acquisition requires ∿ 10 ms per event.

For data taking a negative beam of 2.3×10^6 incoming particles per burst (∿ 1.5 s spill) was used, yielding 10^5 inelastic interactions per burst. The first-stage trigger accepts 6.3×10^{-3} of the inelastic interactions with a measured efficiency of 37% for prompt electrons. This number was obtained from a study of conversion electrons in a sample of interaction data. The second-stage trigger reduces the trigger rate further by a factor of 4 and has an efficiency of 70% for single electrons. The dead-time of the data-acquisition system is ∿ 50%, and 80 triggers per burst are recorded onto tape.

The acceptance of the spectrometer for an electron originating from a semileptonic D decay and for two hadronic decay modes of neutral D's is shown in fig. 2. For the semileptonic D decay we assume an equal rate of decay into K and K^*.

Results are presented on the analysis of 5.9 million triggers at 175 GeV, 1.4 million triggers at 200 GeV, and 2.5 million triggers at 120 GeV incoming π^- beam. The 175 and 200 GeV data are analysed together.

3. DATA ANALYSIS

Off-line selection of electrons removes further background mainly from asymmetric γ conversions and Dalitz decays of π^0 and η^0 where the low-energy pair electron is detected in the in-magnet MWPC system: 85% of all events are rejected while keeping 70% of the prompt electrons. The total efficiency factor for finding single electrons, including all cuts from the first-stage trigger to the off-line selection, is 18 ± 6%. This was determined by analysing ρ, ω, and ϕ signals observed in the data selected with an e^+e^- trigger and by studying conversion pairs from calibration data. We estimate that the data sample selected for final analysis contains 2 to 5% of events with an electron from charm decay.

Charged hadrons are reconstructed with an efficiency of 95% per track. A good knowledge of the mass resolution and the mass scale in invariant mass spectra is essential in this experiment to distinguish charm signals on a large combinatorial background. We therefore checked acceptance, mass scale, and mass resolution thoroughly, using two-body decays of known particles such as ρ, K^0_S, ϕ, Λ, and in particular $\sim$ 150,000 $(\bar{K})^{*0} \to K^{\pm}\pi$ decays measured in our experiment. The mass resolution for $(K + n\pi)$ states in the D-meson mass region differs significantly for the cases where (i) all particles go through both magnets, e.g. $\sigma_m(D^0 \to K\pi)$ = = 10 MeV at the D^0 mass or (ii) only the kaon goes through both magnets (necessary for particle identification) and one (or more) of the pions traverses only the first magnet, e.g. $\sigma_m(D^0 \to K\pi)$ = 22 MeV at the D^0 mass. Data presented in the following are from category (i), unless otherwise mentioned.

Charged particles which pass through the magnet M2 are identified by the three multicellular Čerenkov counters C1, C2, and C3. The pulse-height information from the cells of the Čerenkov counters is used to distinguish π, K, or p in the momentum range 4 to 14 GeV, and to separate unambiguously π, K, and p from 14 to about 75 GeV. Overlap of particles in the Čerenkov cells causes an inefficiency in identification of about 20%. About 35% of the electron-selected events have at least one charged kaon candidate.

These events are further grouped into two samples: those containing an e and a K of the same charge, in the following called "like-sign Ke", are candidates for Cabibbo favoured hadronic charm decay with a K within the charm-decay products; those with an e and a K of opposite charge should not contain such hadronic charm decays.

We have also searched for charm events with hadronic decays containing K^0_S. In reconstructing V^0's we find a K^0_S in 6% of the electron-selected events.

4. CHARM SIGNALS IN MASS SPECTRA

4.1 175 and 200 GeV data

We observe production of D^* mesons decaying into $D\pi$, making use of the very small Q value in this cascade to suppress background, and we see also neutral and

charged D mesons in inclusive mass spectra in five different channels. Wherever possible we require the charm signature of like-sign charge kaon and electron.

4.1.1 The channel $D^* \to D\pi$

Figure 3 shows a scatter plot and projections of $m(K^{\pm}\pi^{\mp})$ versus the mass difference $\Delta m = m(K^{\pm}\pi^{\mp}\pi^{\mp}) - m(K^{\pm}\pi^{\mp})$ for the like-sign Ke data sample. A narrow peak of 28 events on a background of 22 events is observed in the overlap region of a band $142 < \Delta m < 149$ MeV with a band around the D^0 mass $1840 < m(K\pi) < 1890$ MeV. The histograms in fig. 3 show projections of the two bands in a finer binning. The solid lines are fits parametrizing the data by a smooth background and a Gaussian. The fit yields $m(D^0) = (1863.6 \pm 2.4)$ MeV and $\Delta m(D^* - D^0) =$ $= (145.5 \pm 0.3)$ MeV in agreement with the values measured at SPEAR [11]: $m(D^0) = (1864.7 \pm 0.6)$ MeV and $\Delta m(D^* - D^0) = (145.4 \pm 0.2)$ MeV. The fitted resolutions are $\sigma_m = (8.8 \pm 2.4)$ MeV and $\sigma_{\Delta m} = (0.6 \pm 0.2)$ MeV in agreement with values calculated from the known resolution of coordinate and momentum measurement. As expected for charm, no signal is observed in the equivalent scatter plot for the unlike-sign Ke data sample.

We also observe $D^{*\pm}$ production with the $\overset{(-)}{D}{}^0$ decaying into $K^{\pm}\pi^{\mp}\pi^{\pm}\pi^{\mp}$ when applying an x_F cut to the $K\pi\pi\pi\pi$ system. At $x_F(K\pi\pi\pi\pi) > 0.5$ a significant signal (14 signal over 16 background events) is seen at the D^0 mass in the $K\pi\pi\pi$ mass spectrum (here the pions are not requested to go through both magnets) and at the $D^* - D^0$ mass difference in the Δm plot (see also ref. [8]). The fitted mass and mass difference are $m(D^0) = (1857 \pm 9)$ MeV and $m(D^*) - m(D^0) = (145.1 \pm 0.5)$ MeV.

4.1.2 Inclusive $\overset{(-)}{D}{}^0$ and $D^{\pm}$ production

A search for charm signals in inclusive spectra is more difficult than in a decay cascade owing to the high combinatorial background, in particular in the case of high multiplicity channels. We have investigated the channels $K^{\pm}\pi^{\mp}$, $K^{\pm}\pi^{\mp}\pi^{\mp}$, $K^{\pm}\pi^{\mp}\pi^{\pm}\pi^{\mp}$, $K^{\pm}\pi^{\mp}\pi^{\pm}\pi^{\mp}\pi^{\mp}$, $K^{*0}\rho^0$, K^+K^-, $K^0_S\pi^{\pm}$, and $K^0_S\pi^{\pm}\pi^{\mp}\pi^{\pm}$. We find charm signals in five different channels: $K^{\pm}\pi^{\mp}$ (for $x_F > 0.2$), K^+K^- (for $x_F > 0.4$), $K^{\pm}\pi^{\mp}\pi^{\mp}$ (for $x_F > 0.4$), $K^{*0}\rho^0$ (for $x_F > 0.5$) and $K^0_S\pi^{\pm}\pi^{\mp}\pi^{\pm}$ (for $x_F > 0.4$). In fig 4 the combined mass spectra for $\overset{(-)}{D}{}^0$ channels and $D^{\pm}$ channels are shown.

Parametrizing the data by a smooth background and a Gaussian yields $m(\overline{D}^0) =$ $= (1861 \pm 2)$ MeV and $m(D^{\pm}) = (1869 \pm 3)$ MeV with the expected width of $\sigma \approx 10$ MeV.

The non-observation of charm signals above background in the other channels listed above is in agreement with the number of D decays expected in these channels from the observed signals, using measured branching ratios [11], estimates of efficiencies for K^0_S reconstruction, and relative acceptance of the different channels.

4.2 120 GeV data

The data taken at 120 GeV correspond to 40% of the microbarn equivalent of the 175 and 200 GeV data. A small $D^{*\pm} \to \overline{D}^0\pi^{\pm}$ signal is observed in both the $D^0 \to K\pi$ (3 signal over 2 background events) and $D^0 \to K\pi\pi\pi$ decay channels (9 signal over 4 background events). Figure 5 shows D^0 mass and $D^* - D^0$ mass difference distributions for the $D^0 \to K\pi\pi\pi$ channel for $x_F(D^*) > 0.5$. The fitted mass and mass difference are $m(D^0) = (1866 \pm 10)$ MeV, $\Delta m(D^* - D) = (145.1 \pm 1.8)$ MeV.

In inclusive mass spectra no significant D-meson signals are seen.

5. CROSS-SECTION

To determine the $D\overline{D}$ cross-section we use the inclusive $\overline{D}^0 \to K^{\mp}\pi^{\pm}$ and $D^{\pm} \to K^{\mp}\pi^{\pm}\pi^{\pm}$ signals at 175 and 200 GeV which give the best determination of the x_F and p_T^2 distribution [8]: $d^2\sigma/dx_F dp_T^2 \propto (1 - |x_F|)^{0.8}\, e^{-1.1 p_T^2}$. Since the type, the particular decay mode, and the x_F and p_T^2 distributions of the semileptonically decaying charmed particles cannot be measured in this experiment, we make the following assumptions about the production mechanism:

i) There is only D and D^* production.

ii) Each D of a $D\overline{D}$ pair is produced independently with the same x_F and p_T^2 distribution.

iii) D mesons decay semileptonically via K and K^* at equal rate.

iv) Linear A dependence of the cross-section.

Table 1 summarizes the values used for the calculation of the total cross-section. With this input we evaluate an inclusive cross-section

$$\sigma(D\overline{D} + X) = (48 \pm 15)\ \mu b \text{ per nucleon}$$

for the 175 and 200 GeV data, where the error is statistical only. We have an additional normalization uncertainty of 50%, half of which is due to the errors in the branching ratios and the other half to the error in the efficiency in finding the electron.

We next consider how the result for the integrated cross-section depends on the exponent of the x_F distribution used to extrapolate into the region below $x_F = 0.2$ and on possible correlations between charmed particles. The inclusive $K^{\pm}\pi^{\mp}$ data, in which π's pass through the first magnet only, are the sample with good acceptance in the small x_F region $0 < x_F < 0.2$. We therefore use these data, in which no charm signal is observed, to determine a 95% C.L. upper limit for a possible additional central charm component with $d\sigma/dx_F \propto (1 - x_F)^6$ [4]. Such a component would, at the upper limit, increase our $D\bar{D}$ cross-section by 50%. To estimate the influence of an x_F distribution not symmetric around $x_F = 0$ on the cross-section (e.g. on x_F distribution for D production decreasing for $x_F < 0.2$ as is the case in ψ production by π's [13]), we have assumed that the x_F distribution goes linearly to zero in the interval $x_F = 0.2$ to $x_F = -1$. In this case our value for $\sigma(D\bar{D})$ would decrease by 20%. Extreme cases of short- and long-range correlations between the two D's of a pair, which are still consistent with our observations, can change the cross-section by factors ranging from 0.5 to 1.7.

The ratio of the cross-sections at the two energies can be measured with better accuracy than the absolute cross-section due to cancellation of some systematic errors; it is

$$\sigma(D\bar{D})\ [120\ \text{GeV}]/\sigma(D\bar{D})\ [175/200\ \text{GeV}] = 0.62 \pm 0.34\ .$$

The value of the cross-section at 175 and 200 GeV is an order of magnitude larger than predicted on the basis of perturbative QCD calculations, including quark- and gluon-fusion diagrams [14]. However, models including non-perturbative flavour excitation diagrams [15] have obtained a value and energy dependence of the cross-section in agreement with our observations.

Acknowledgements

We would like to acknowledge the contribution of the SPS crew and services to the success of this experiment. The help of the SPS Experimental Area group in setting up the beam was invaluable. We also wish to express our thanks for the many important contributions of the technical staff of the participating institutes. The members of the Cracow group would like to thank MPI, CERN, and NIKHEF-H for their support and hospitality.

REFERENCES

[1] G. Goldhaber et al., Phys. Rev. Lett. 37 (1976) 255.

[2] A. Bodek et al., Univ. Rochester preprint UR-827, COO-3065-335 (1982).
M. Jonker et al., Phys. Lett. 96B (1980) 435.
H. Wachsmuth, Proc. Symposium on Lepton and Photon Interactions at High Energy, Batavia, 1979 (FNAL, Batavia, 1980), p. 551.
T. Hansl et al., Phys. Lett. 74B (1978) 139.
S. Chilingarov et al., Phys. Lett. 83B (1979) 136.

[3] J. Sandweiss et al., Phys. Rev. Lett. 44 (1980) 1104.
H. Fuchi et al., Phys. Lett. 85B (1979) 135.
A. Badertscher et al., Phys. Lett. 123B (1983) 471.

[4] M. Aguilar-Benitez et al., Phys. Lett. 123B (1983) 98 and 103.

[5] K.L. Giboni et al., Phys. Lett. 85B (1979) 437.
W. Lockman et al., Phys. Lett. 85B (1979) 443.
D. Drijard et al., Phys. Lett. 81B (1979) 250.
A.N. Aleev et al., The study of Λ_c^+ charm baryon production in a 58 GeV neutron beam, Contribution to the 21st Int. Conf. on High Energy Physics, Paris, 1982.
L.J. Koester et al. Proc. 20th Int. Conf. on High Energy Physics, University of Wisconsin, Madison, 1980 (Amer. Inst. Phys., New York, 1981), p. 190.
S.F. Biagi et al., Observation of a narrow state at 2.6 GeV/c^2, a candidate for the charmed strange baryon A^+, submitted to Phys. Lett. B.

[6] V.L. Fitch et al., Phys. Rev. Lett. 46 (1981) 761.

[7] J.W. Cooper, *in* Proc. 16th Rencontre de Moriond, Les Arcs, Savoie, 1981 (Editions Frontières, Dreux, 1981).
M. Basile et al., Nuovo Cimento 63A (1981) 230, 65A (1981 457, 67A (1982) 40.

[8] R. Bailey et al., Production and decay properties of D and D^* mesons in π^-Be interactions, submitted to Phys. Lett. B.

[9] W. Spierenburg, Ph.D. Thesis, Charmed baryon search in hadronic interactions with 150 GeV/c incident protons, NIKHEF-H, Amsterdam, 1983.

R. Jongerius, Ph.D. Thesis, Single and double ϕ production in hadronic interactions at 100 and 175 GeV/c, NIKHEF-H, Amsterdam, 1982.

[10] C. Damerell et al., Comput. Phys. Commun. 22 (1981) 349.

[11] Particle Data Group, Review of particle properties, Phys. Lett. 111B (1982).

[12] R.H. Schindler et al., Phys. Rev. D 24 (1981) 78.

[13] J. Badier et al., Phys. Lett. 86B (1979) 98.

[14] J. Babcock et al., Phys. Rev. D 18 (1978) 162.

[15] B. Combridge, Nucl. Phys. B151 (1979) 429.

F. Halzen, Proc. 21st Int. Conf. on High Energy Physics, Paris, 1982, J. Phys. 43, Suppl. 12, C-3, 381 (1982).

Table 1

Values used for the calculation of the cross-section

$N_{obs}(\bar{D}^0 \to K^{\mp}\pi^{\pm})$ with $x_F > 0.2$	115 ± 34
$N_{obs}(D^{\pm} \to K^{\mp}\pi^{\pm}\pi^{\pm})$ with $x_F > 0.4$	89 ± 31
$N(\pi$ incoming)	1.01×10^{11}
$[\text{Luminosity}]^{-1}$ [μb/(nucleon·event)]	2.9×10^{-6}
$BR(\bar{D}^0 \to K^{\mp}\pi^{\pm})$ [11]	(2.4 ± 0.4)%
$BR(D^{\pm} \to K^{\mp}\pi^{\pm}\pi^{\pm})$ [11]	(4.6 ± 1.1)%
$BR(D^0 \to e + X)$ [12]	(5.5 ± 3.7)%
$BR(D^{\pm} \to e + X)$ [11]	(19 ± 4)%
$N_{prod}(D^0)/N_{prod}(D^{\pm})$ [8]	1.4 ± 0.8
Acc $(D \to e + K/K^* + X)$	9.5%
Acc $(D^0 \to K\pi)$, $x_F > 0.2$	12.7%
Acc $(D^{\pm} \to K\pi\pi)$, $x_F > 0.4$	7.4%

Figure captions

Fig. 1 : a) ACCMOR forward spectrometer (top view);

b) Layout of the electron trigger system (top view).

Fig. 2 : Acceptance of the spectrometer for D decays including geometry, particle identification, and reconstruction efficiency. Solid curve: $D \to eX$. Dashed curve: $D^0 \to K\pi$. Dotted curve: $D^0 \to K\pi$ with K and π passing through both magnets (best mass resolution sample; see Section 3). Dashed-dotted curve: $D^0 \to K\pi\pi\pi$.

Fig. 3 : Scatter plot of mass $m(K^{\pm}\pi^{\mp})$ versus mass difference $m(K^{\pm}\pi^{\mp}\pi^{\mp}) - m(K^{\pm}\pi^{\mp})$ for the like-sign Ke data sample with best mass resolution. The projections of the bands are in smaller binning. Curves are fits parametrizing the data with a Gaussian plus a polynomial for the background.

Fig. 4 : Inclusive mass spectra. The fits parametrize the data with a Gaussian plus a polynomial.

a) Combined mass spectra for three $\overset{(-)}{D}{}^0$ decay channels:
$\overset{(-)}{D}{}^0 \to K^{\mp}\pi^{\pm}$ for $x_F > 0.2$, $\overset{(-)}{D}{}^0 \to K^{*0}\rho^0$ for $x_F > 0.5$,
$\overset{(-)}{D}{}^0 \to K^+K^-$ for $x_F > 0.4$.

b) Combined mass spectra for two $D^{\pm}$ decay channels:
$D^{\pm} \to K^{\mp}\pi^{\pm}\pi^{\pm}$ for $x_F > 0.5$, $D^{\pm} \to K^0_S\pi^{\pm}\pi^{\mp}\pi^{\pm}$ for $x_F > 0.4$.

Fig. 5 : Projections of bands in the scatter plot of mass $m(K^{\pm}\pi^{\mp}\pi^{\pm}\pi^{\mp})$ versus mass difference $\Delta m = m(K^{\pm}\pi^{\mp}\pi^{\pm}\pi^{\mp}\pi^{\mp}) - m(K^{\pm}\pi^{\mp}\pi^{\pm}\pi^{\mp})$, for the like-sign Ke data sample at 120 GeV with a cut on $x_F(K4\pi) > 0.5$. The bands selected are $1.845 < m_{K\pi\pi\pi} < 1.885$ and $143 < \Delta m < 148$ MeV. The fits parametrize the data with a Gaussian plus a polynomial.

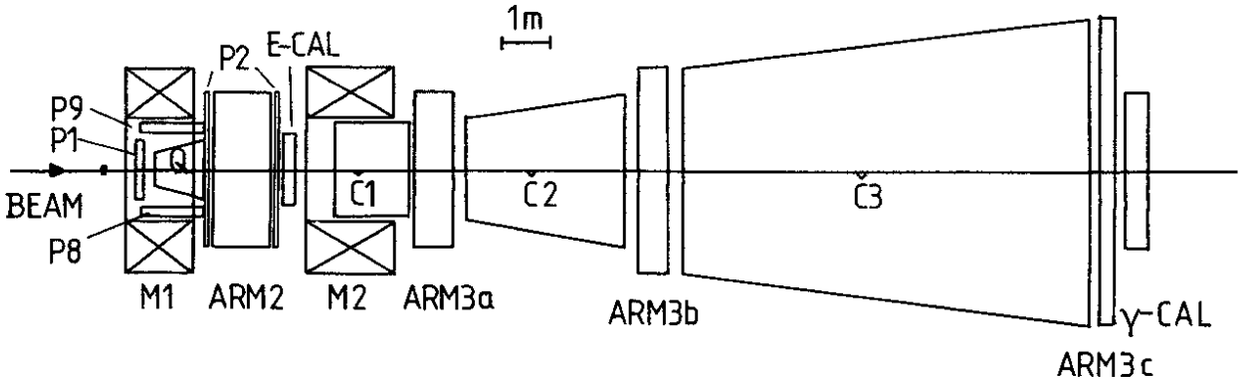
1m
P2
E-CAL
P9
P1
Q
BEAM
P8
C1
C2
C3
M1
ARM2
M2
ARM3a
ARM3b
γ-CAL
ARM3c

a)

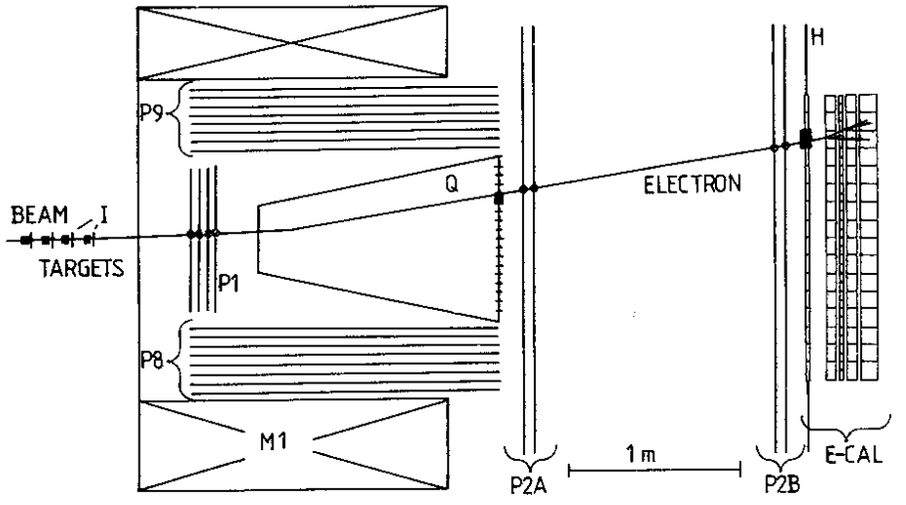
H
P9
Q
ELECTRON
BEAM
I
TARGETS
P1
P8
M1
1m
E-CAL
P2A
P2B

b)

Fig. 1

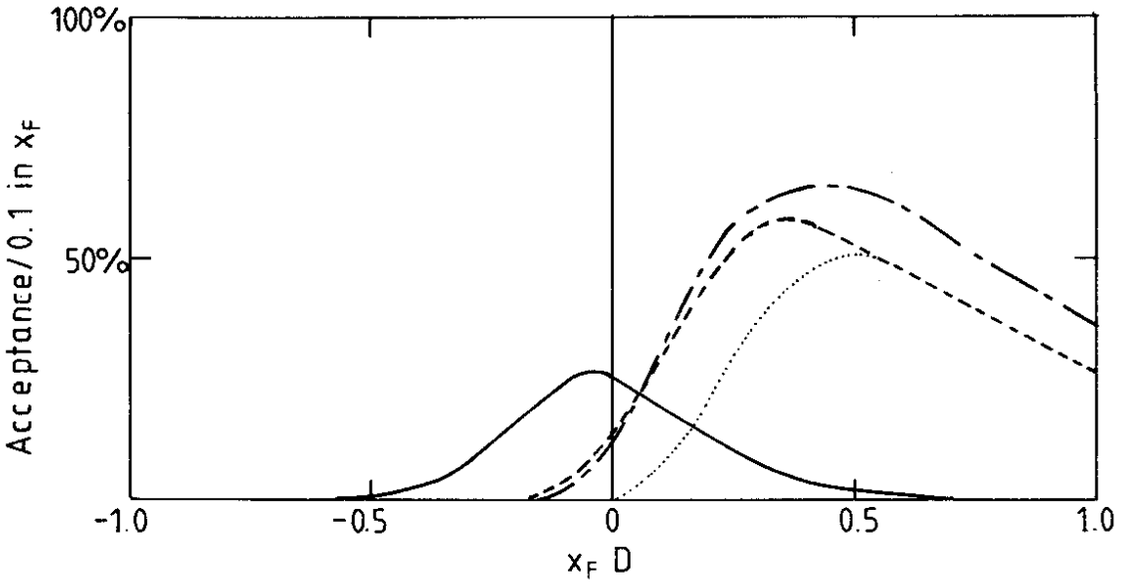
100%
50%
Acceptance/0.1 in x_F
-1.0
-0.5
0
0.5
1.0
x_F D

Fig. 2

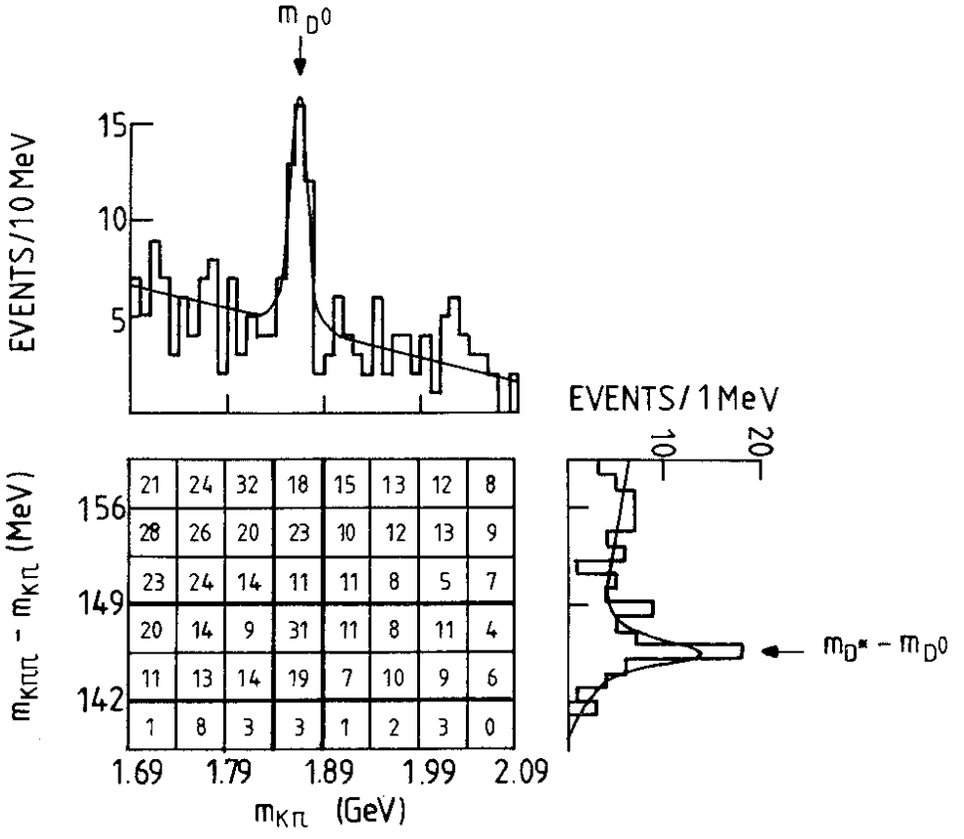
m_{D^0}
EVENTS/10 MeV
15
10
5
EVENTS/1 MeV
10
20
$m_{D^*} - m_{D^0}$
$m_{K\pi\pi} - m_{K\pi}$ (MeV)
156
149
142
21 24 32 18 15 13 12 8
28 26 20 23 10 12 13 9
23 24 14 11 11 8 5 7
20 14 9 31 11 8 11 4
11 13 14 19 7 10 9 6
1 8 3 3 1 2 3 0
1.69
1.79
1.89
1.99
2.09
$m_{K\pi}$ (GeV)

Fig. 3

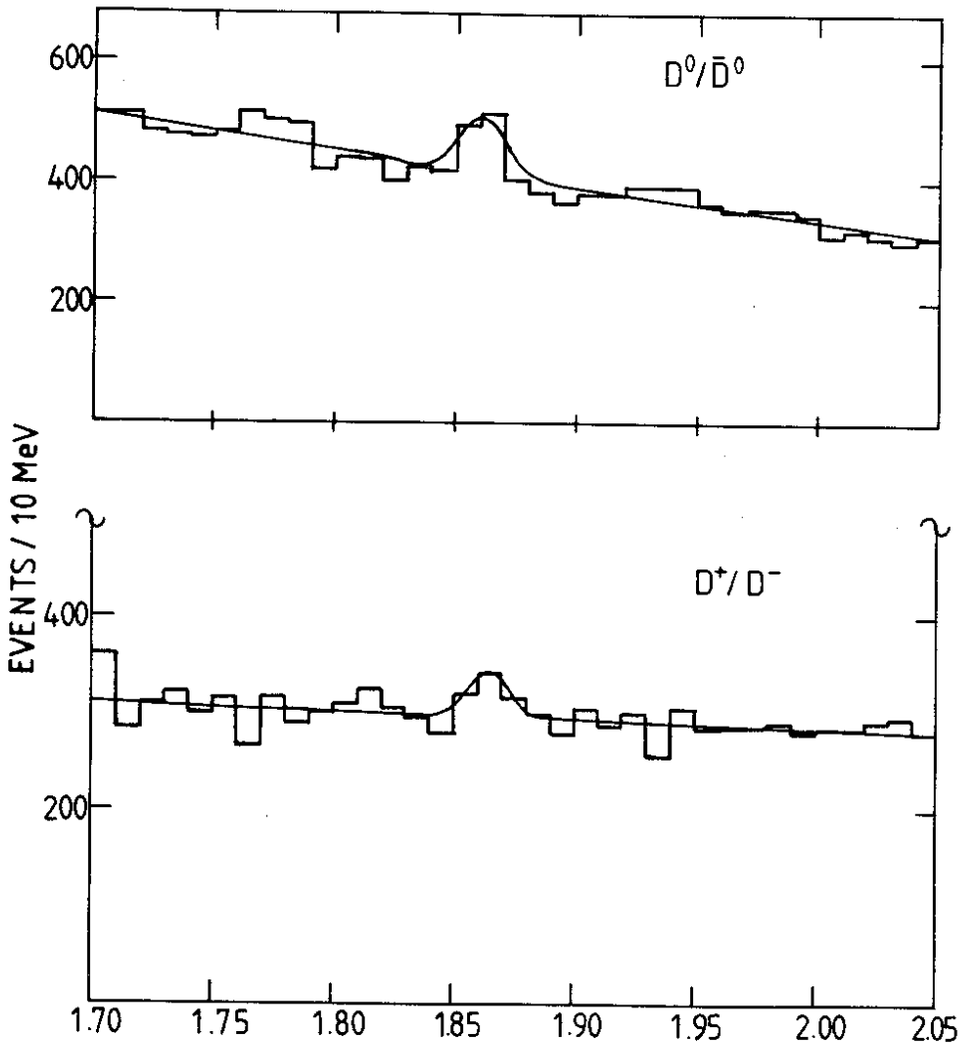
600
400
200
$D^0/\bar{D}^0$
EVENTS / 10 MeV
400
200
D^+/D^-
1.70
1.75
1.80
1.85
1.90
1.95
2.00
2.05

Fig. 4

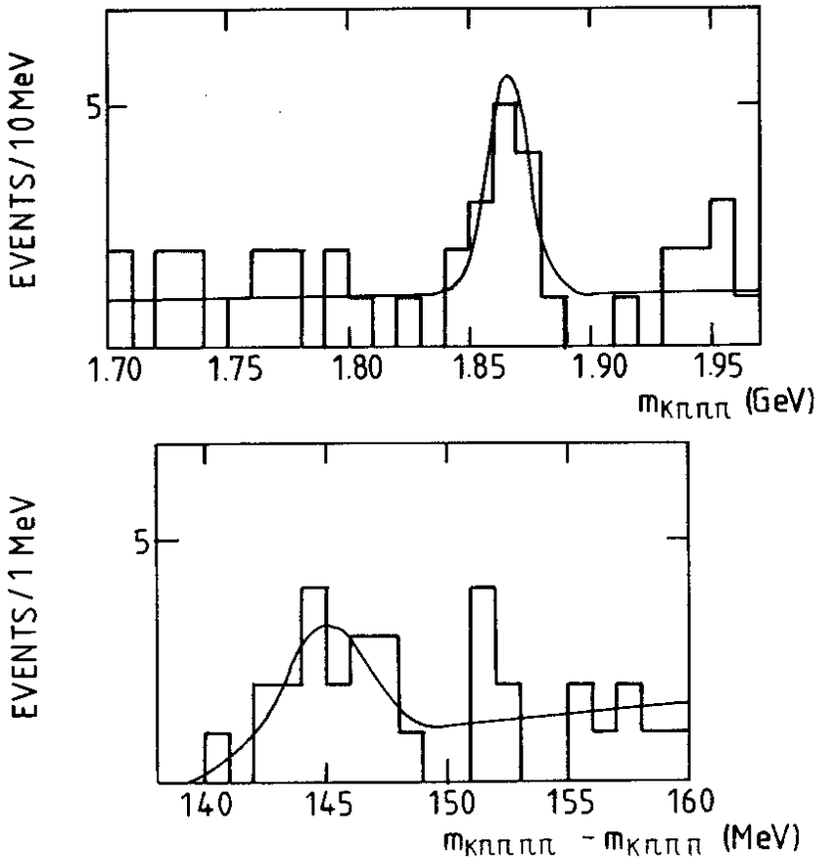
EVENTS/10MeV
5
1.70
1.75
1.80
1.85
1.90
1.95
$m_{K\pi\pi\pi}$ (GeV)
EVENTS/1 MeV
5
140
145
150
155
160
$m_{K\pi\pi\pi\pi} - m_{K\pi\pi\pi}$ (MeV)

Fig. 5